scientific reports

Check for updates

OPEN

Finite element analysis of stress in removable lower complete denture under vertical and oblique occlusal forces

Yassine Madoune[1,2]✉, Jarosław Żmudzki[1]✉ & Hyeonjong Lee[3]

Frequent fractures of complete removable dentures during mastication in the anterior zone cannot be explained by bite forces in this area, because occlusal forces on the incisors are small. It appears that the mechanism of fracture must be from lateral mastication forces. The hypothesis of the study was that, under stable support of a complete removable denture on the foundation, its fracture in the anterior segment is possible due to stress generated under masticatory forces typical for denture wearers. This study analyzes stress distribution in removable complete dentures (designed in Exocad), using the finite element method (FEM, Nx Siemens). The denture was loaded on the first molars with bilateral vertical forces of 100 N and oblique forces of 140 N at an angle of 45°. Under oblique bilateral mastication forces the anterior zone exhibited nominal stresses originating from tension on the lingual side and compression on the labial side. These values were significantly lower than the material's strength, even under conservative criteria for semi-brittle polymer in tension-dominant zones. The study also showed that the stress in properly manufactured dentures without defects or excessively sharp grooves did not reach the fatigue strength of the denture materials. This negated the hypothesis that denture fracture in the anterior segment is possible under such conditions. Further investigation is required, incorporating factors such as denture foundation resiliency, misfit, occlusal imbalance, and potentially different loading patterns to fully elucidate intraoral failure modes.

Keywords Denture, Fracture, Strength, Finite element analysis, Force, Stress, Load bearing capacity

Removable complete dentures, supported by soft tissue without implants, are a conventional prosthetic option for fully edentulous patients. These dentures depend entirely on the oral mucosa covering the residual alveolar process[1]. Their biomechanical performance under masticatory forces is crucial for durability, patient comfort, and preventing fractures, which is why the strength of denture base materials is a key property that research focuses on. Unfortunately, many dentures fracture, occurring in 20–30% of cases, approximately half due to impact and half during intraoral service[2–5]. Impact fracture is self-explanatory, but there is a significant problem with fractures during chewing. Experimental studies of denture load-bearing capacity require forces significantly exceeding the maximum human occlusal forces to achieve fracture[2,6]. Moreover, dentures mainly break in the anterior section during chewing[4,7]. Meanwhile, it is worth noting that according to the basics of prosthetics, it is impossible to generate significant forces in the anterior zone in removable dentures, and only balancing the denture wings allows for achieving forces sufficient for food mastication in the lateral zones[8]. This is also confirmed by clinically performed occlusal force measurements[9,10].

A paradox arises because dentures fracture in the anterior region, where occlusal forces are minimal, and explaining this phenomenon through experiments or simulations requires excessively large forces or conditions facilitating fracture. Stress distribution, deformation, and load bearing capacity of complete dentures are analyzed using the finite element method (FEM)[11]. FEA of the stress state in the dentures requires the introduction of very deep anatomical undercuts[12] or material defects[13], around which the stresses increase to levels justifying fracture. Simulation tests taking into account the mandibular movement[14] also require forces exceeding the values achieved by denture wearers. Another concept is the introduction of selective support of the denture with a load above the fracture zone[15]. The result of the stress value in FEM is strongly influenced by the size of

[1]Department of Engineering Materials and Biomaterials, Faculty of Mechanical Engineering, Silesian University of Technology, 18a Konarskiego Str., Gliwice 41–100, Poland. [2]Doctoral School, Silesian University of Technology, 2A Akademicka Str., Gliwice 44–100, Poland. [3]Department of Prosthodontics, College of Dentistry, Yonsei University, Seoul, South Korea. ✉email: Yassine.Madoune@polsl.pl; Jaroslaw.Zmudzki@polsl.pl

the finite elements. In older studies, due to limited computer power, the finite elements were relatively large[16,17]. In some analyses, attention is paid to the size of finite elements or at least their number is given[11,15]. However, the exact size of finite elements in the region of interest is not given, and no study of the effect of element size on the stress result is presented. Therefore, it is not known whether the stress value converges to the exact value of the model according to the principles of FEM simulation studies. Inadequate mesh refinement underestimates stress values; thus, this study aimed to assess stress convergence under clinically relevant bite forces (100–140 N). Additionally, as masticatory efficiency depends on denture stabilization, support conditions in the model should align with prosthodontic principles.

The hypothesis of the study was that, under stable support of a complete removable denture on the foundation, its fracture in the anterior segment is possible due to stress generated under masticatory forces typical for denture wearers.

Methods

The geometry of a lower complete denture was designed using dental CAD software (Exocad DentalDB ver.3.2, Exocad GmbH, Darmstadt, Germany, https://exocad.com/), ensuring accurate representation of prosthetic features. The model was exported and imported as a surface triangular mesh (STL) with standard default settings into engineering CAD software (NX Siemens PLM Software ver.2312, Plano, TX, USA, https://plm.sw.siemens.com/en-US/) for preprocessing and finite element analysis (Figs. 1 and 2). A mucosal layer with a thickness of about 2 mm was generated by offsetting the mucosal surface in cad software (Nx Siemens).

The boundary conditions were set by completely fixing the movement of the basal mucosal surfaces that touch the alveolar ridge. This setup replicated the mucosa's adherence to and support by the underlying rigid bone. Bone elastic modulus (10–20 GPa) is several orders of magnitude higher than that of the soft tissues, and bone deformation under denture loading can be considered negligible (rigid body) compared to mucosal strain[18]. The edges of mucosa were left free to move naturally when load was applied.

All materials were modeled with linear elastic behavior to focus on the influence of mesh density.

The denture material was designated a Young's modulus of 2000 MPa and a Poisson's ratio of 0.3, indicative of standard characteristics of acrylic-based denture materials (Table 1). The mucosa was characterized by a Young's modulus of 5 MPa and a Poisson's ratio of 0.45 to replicate its compliant behavior[19]. Denture to mucosa interface was modeled with perfect adhesion (bonded contact) and no sliding or separation behavior was assigned emulating perfect denture stability. The artificial teeth were integrated into the denture (not modeled as separate parts), what reflects conventional denture fabrication processes using base and tooth materials with similar moduli of elasticity.

Two loading scenarios were simulated to emulate functional occlusal forces:

- Vertical loading: A symmetrical bilateral vertical force of 100 N was exerted on the molar cusps.

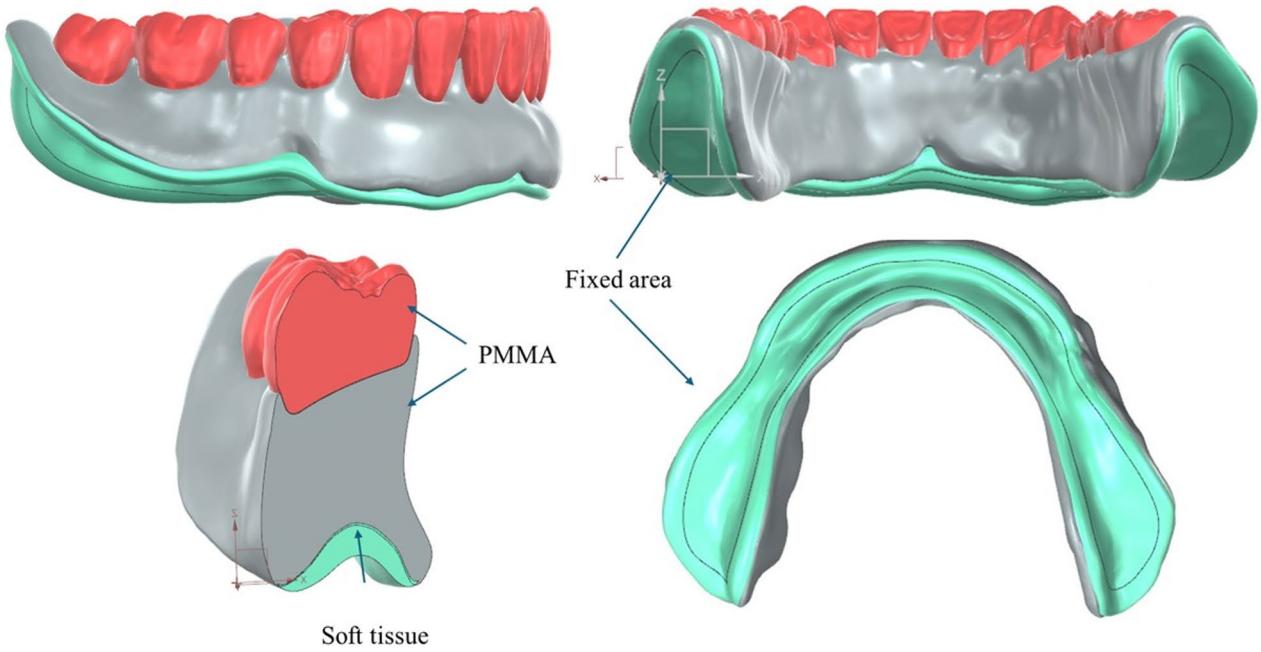

Fig. 1. View of CAD model (NX Siemens) after import of STL model from dental CAD (Exocad) and cross-sectional schematic through the first molar region showing model layers: denture base and artificial teeth (the same PMMA material), mucosa, and fixation area on bone (bone as rigid body excluded in FEA).

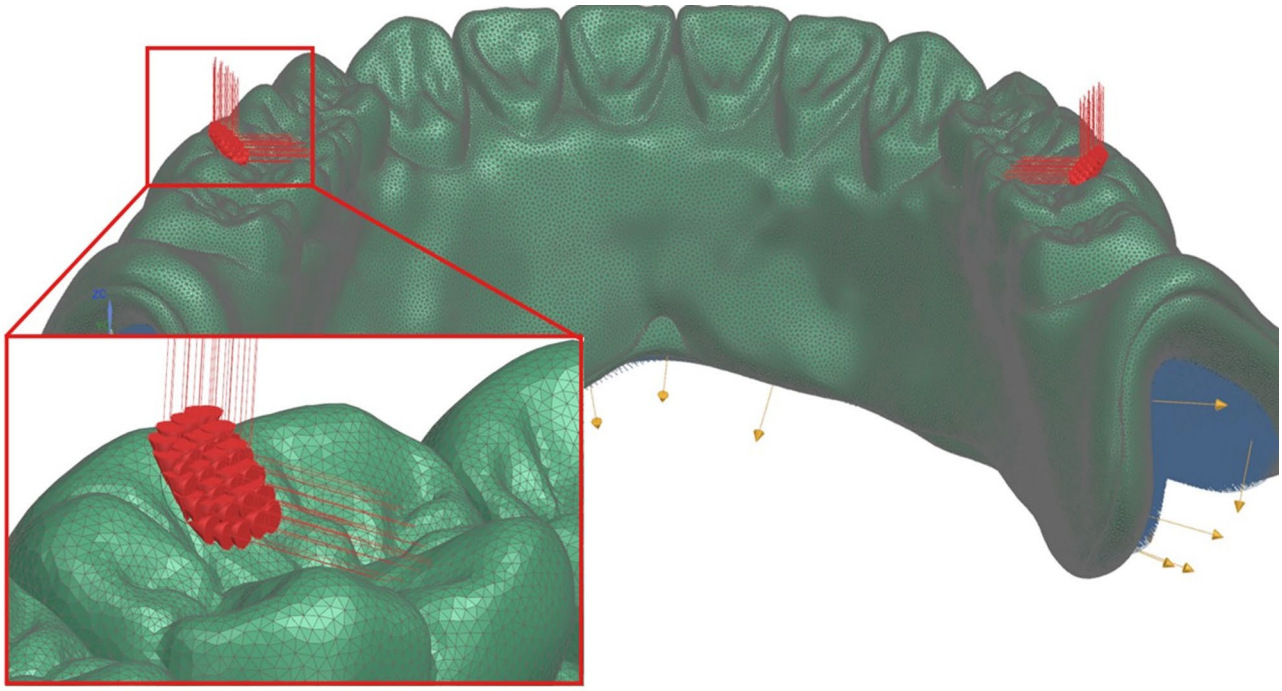

Fig. 2. FEM model of lower removable complete denture on soft tissue and loading area of first molar cusps with vertical 100 N and oblique 140 N symmetric forces (mesh size 0.3 mm).

Component	Young's Modulus (MPa)	Poisson's ratio
Denture (PMMA)	2000	0.30
Mucosa	5	0.45

Table 1. Mechanical properties of materials.

Mesh size	Number of elements	Number of nodes
0.8 mm	~ 209,581	~ 325,358
0.5 mm	~ 651,669	~ 971,415
0.3 mm	2,301,576	3,326,502

Table 2. Mesh characteristics.

- Oblique loading: The vertical load of 100 N was supplemented with a horizontal force of 100 N given externally to the dental arch to replicate lateral masticatory forces, resulting in a bilaterally resultant oblique (45˚) forces of 140 N on each side.

Three mesh densities levels were created to assess convergence of stress results (Table 2): coarse (0.8 mm element size), medium (0.5 mm), and fine (0.3 mm). Tetrahedral 2nd order elements (10-node) were employed across all models to ensure computational efficiency while maintaining accuracy. Finally, after achieving mesh convergence for the nominal stress value, local mesh refinement[20] to sizes 0.15 mm and 0.1 mm was implemented to systematically assess the influence of element size on stress value in and around the assumed sharp anatomical groove in the criterion anterior zone (presented in Results section for clearance). Finite element analysis (FEA) was performed to assess equivalent Huber-Mises-Hencky stress (eqvHMH-according to maximum distortional strain energy density Huber-Mises-Hencky theory) and principal stresses distribution.

Results

Oblique forces caused significantly higher stresses than vertical forces in a way disproportionate to 40% difference in their values - Fig. 3.

Convergence analysis revealed that elemental and nodal eqvHMH stress distributions were uniform and very similar for all meshes, with the only differences occurring locally around sharp undercuts and grooves-

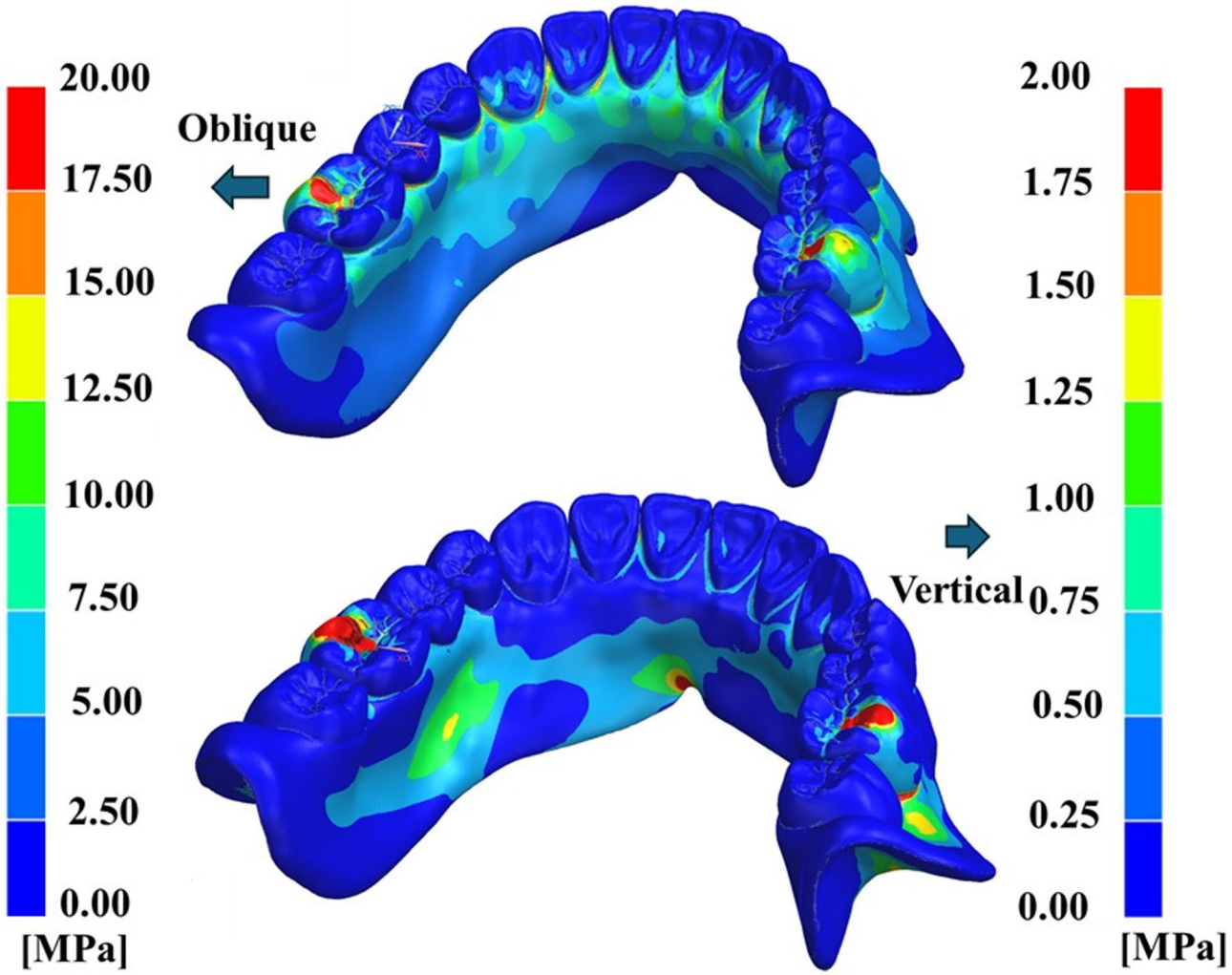

Fig. 3. Equivalent Huber-Mises-Hencky nodal stress value under bilateral oblique 140 N forces and vertical 100 N.

Figs. 4 and 5. The finest mesh (0.3 mm) provided the highest resolution without significant discrepancies and the detection of stress field edges was visible smoother compared to coarser meshes (0.5 mm and 0.8 mm).

Stress concentrations immediately adjacent to the loading nodes on molar cusps were identified as finite element method (FEM) artifacts (Fig. 4 – "A") and excluded from further analysis. Stress values in molar tooth were assessed in deeper regions beneath the loaded cusps, beyond the influence of these artifacts.

The model is assumed to converge to its exact numerical solution if the stress values for successively smaller elements differ by no more than 10%. For example, for the deeper region, the elemental value with decreasing finite element size was 9.63, 9.05, and 9.34 MPa, while the nodal value was 6.76, 8.87, and 8.95 MPa, respectively. The region between 12.5 and 15 MPa (yellow range at scale) can also be considered stable and quite distant from artifact "A." The elevated stress values were also observed at the lateral side of molar tooth bases in elements in the cervical groove. The elemental value increased from 11.2, 12.5, and 15.8 MPa, while the nodal values increased from 13.1, 13.8 and 17.3 MPa, respectively, across mesh densities (0.8, 0.5 and 0.3 mm). Elevated stress values were also revealed at the anterior segment, as shown in Fig. 5a for the subsequent mesh sizes. Elemental and nodal eqvHMH stress values on the zone between the canine and second incisor tooth were 13.35, 15.62 and 17.61 MPa, and 20.70, 19.87 and 24.65 MPa, respectively.

For comparison, nodal values at the lateral zone between the molar and premolar tooth on the finest mesh (Fig. 5b) were 28.97 and 26.83 MPa. The values are larger than those on the scale because the scale was limited to 20 MPa to avoid reducing the red zone range in the views. However, it should be noted that these are local stress values in finite elements into grooves, whose sizes are similar to the smallest finite elements of 0.3 mm. Finest mesh still was unable to smoothly approximate these shapes, and arrangement of the finite elements was random, and the values were not stable and convergent within 10%. For comparison, elemental and nodal eqvHMH stress values in the area immediately adjacent to the grooves below the canine were stable and convergent, and amounted to 8.86, 9.14, 9.41 MPa, and 9.47, 9.57, 9.58 MPa, respectively (Fig. 5a). To examine how deep the elevated stress zone reaches, similarly to the molar tooth, a cross-section through the canine is presented in

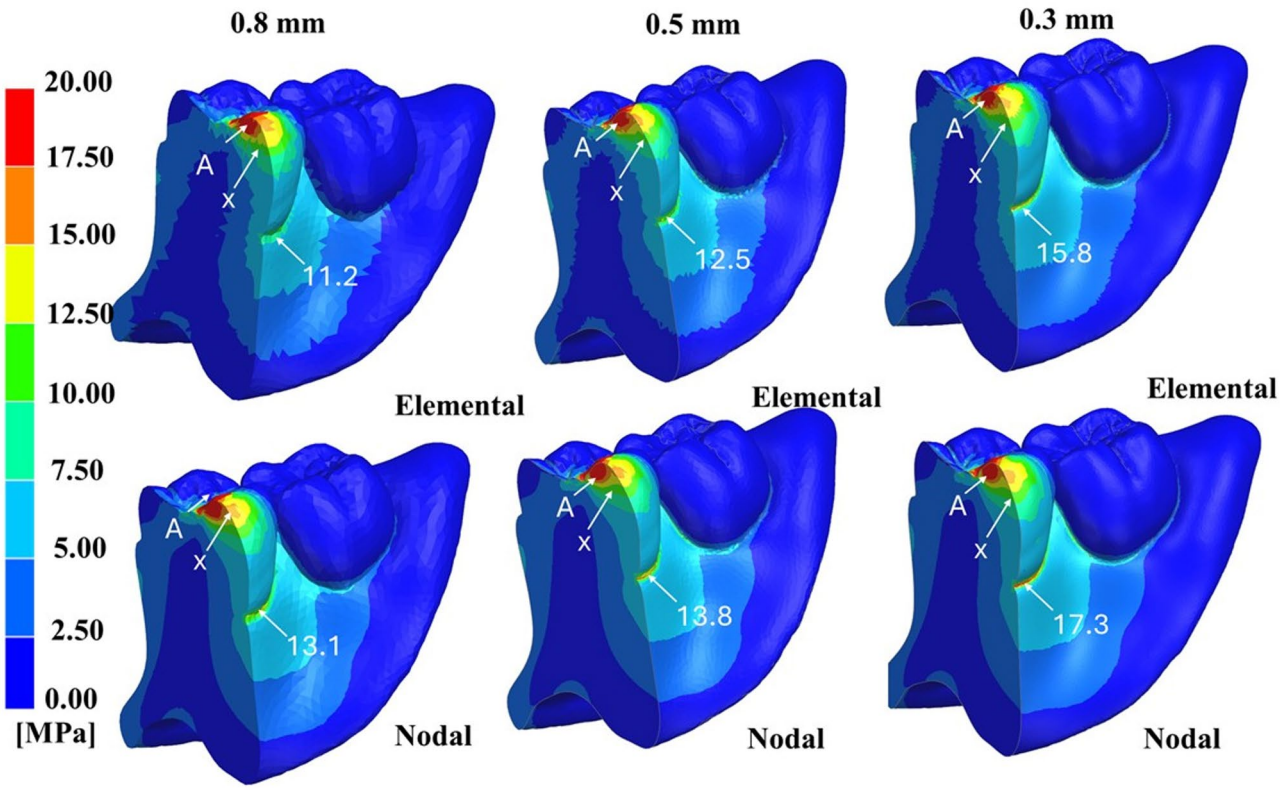

Fig. 4. Elemental and nodal value of equivalent Huber-Mises-Hencky stress in cross-section through loaded first molar tooth regarding to mesh size under bilateral oblique forces 140 N.

Fig. 5c. In contrast to the loaded molar tooth, here the stresses reached very shallowly, and the stress range of 10–12.5.5 MPa was barely visible at the surface, while in the molar cusp was stable and reached at least one scale increment higher, 12.5–15.5 MPa. If we consider values convergent and distant from the uncertain values into grooves, the stress at the anterior segment was lower than inside the molar cusps. Similarly, if we compare values into grooves to those at the posterior critical zones, the stress was higher than in the anterior segment.

In the anterior region, highest eqvHMH stresses were noted at the canines (Fig. 5), particularly on the lingual side, where tensile stresses were higher than in the labial region (Fig. 6). Minimum principal stress reveal that molar tooth was compressed toward lateral direction and also labial side of anterior segment under canine was compressed from bending (Fig. 7).

The highest eqvHMH stress under vertical load was around labial undercut. It came from compression (Fig. 7) and the values reached only a few megapascals. At the same time, the highest maximal principal stress was between incisor grooves (Fig. 6). This showed that the denture under vertical forces was bent in a simple way relative to the plane of the occlusion and the foundation, while under oblique loads it experienced bending and torsion outside relative to the arch.

To better illustrate the complex stress state, Fig. 8 presents the maximum (tension) and minimum (compression) principal stress values together, with a clearly visible boundary between compression and tension. In the cross-section through the incisors, a clear separation between tension on the lingual side and compression on the labial side, characteristic of bending, can be observed. In the cross-section through the canine region, bending is no longer so clearly visible – in the saddle on the lingual slope, tension has disappeared and compression has appeared. Displacements are also presented to better illustrate the directions of deformation, which document that the denture wing is not only bent but also torsion, while the incisor region migrates slightly inward as a result of tension.

Stress analysis showed that molar tooth was more prone to fracture, despite clinical observations of occasional fractures at lateral side and rare moral cusp failure. In this situation, we analyzed the results of local mesh size increments to 0.15 mm and 0.1 mm between the canine and incisor, a region where fractures frequently occur in clinical practice - Fig. 9. Local mesh densification was performed for this area, considering it the primary area of interest because brittle materials are significantly more sensitive to tension, thus omitting the compression region from the local analysis. In the area adjacent to the groove, the nominal stress values remained stable, slightly below 10 MPa (9–9.6.6 MPa) for the 0.15 and 0.1 mm meshes. Within the groove, the nodal values converged between 25 MPa and 27 MPa, and the elemental values were 18 MPa and 19 MPa. Although the stress within the groove did not increase to values critically higher than in the molar tooth area, its influence should be considered because, unlike the molar tooth, it originates from tension. In the concentration zones in the grooves and adjacent areas, we checked the intermediate stresses, but the biaxiality ratio did not exceed 0.5–0.6 in groove

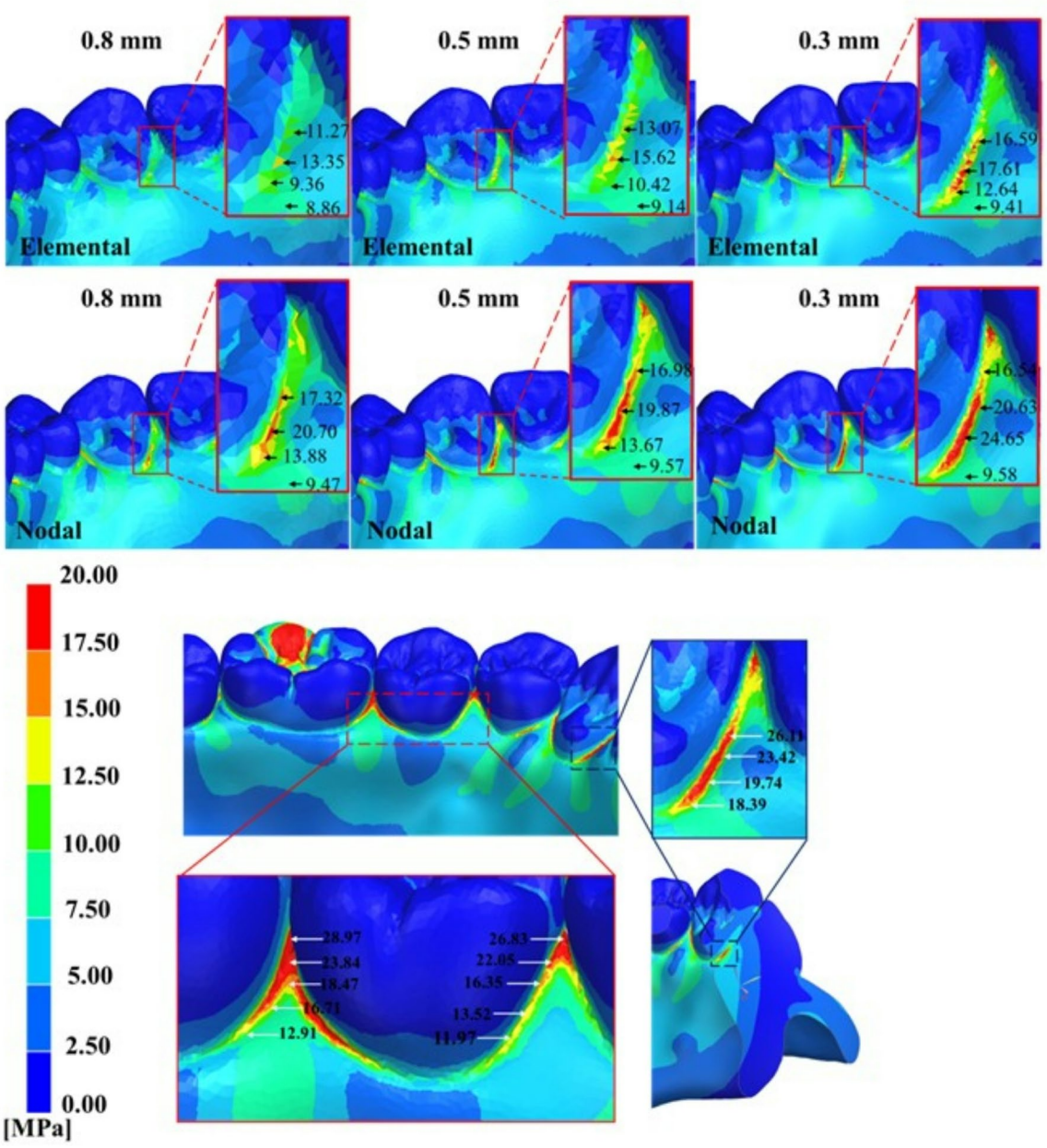

Fig. 5. Elemental and nodal equivalent Huber-Mises-Hencky stress values on the zone between canine and 2nd incisor tooth (**a**) nodal value on lateral zone (**b**) and at cross-section through canine (**c**) under bilateral oblique 140 N forces.

and was very low around groove in adjacent zones. The risk of immediate fracture and fatigue strength has been discussed in more detail depending on the denture material and the application of the appropriate failure theory depending on its sensitivity to stress state.

Discussion

The study showed that stresses under bilateral vertical loading were not criteria for denture fracture and were incomparably lower compared to bilateral oblique force.

The highest eqvHMH stress value with clear convergence to the exact solution was observed inside the loaded molar tooth and reached 15 MPa inside the cusp at a distance of several finite elements below the nodes loaded with occlusal force. We physically applied the occlusal force over a relatively large surface area to reduce the effect of overestimating displacements at the loaded nodes. However, we decided not to consider these values and assumed a significant distance from the loaded nodes to avoid overestimating stresses and preferred to take lower stresses, as we were looking for causes of fractures through the anterior part. Here, on the lingual side of anterior saddle the convergent stress value was up to 10 MPa at a sufficient distance from the disturbances on local grooves. This observation challenges the hypothesis that mesh refinement would reveal critical anterior

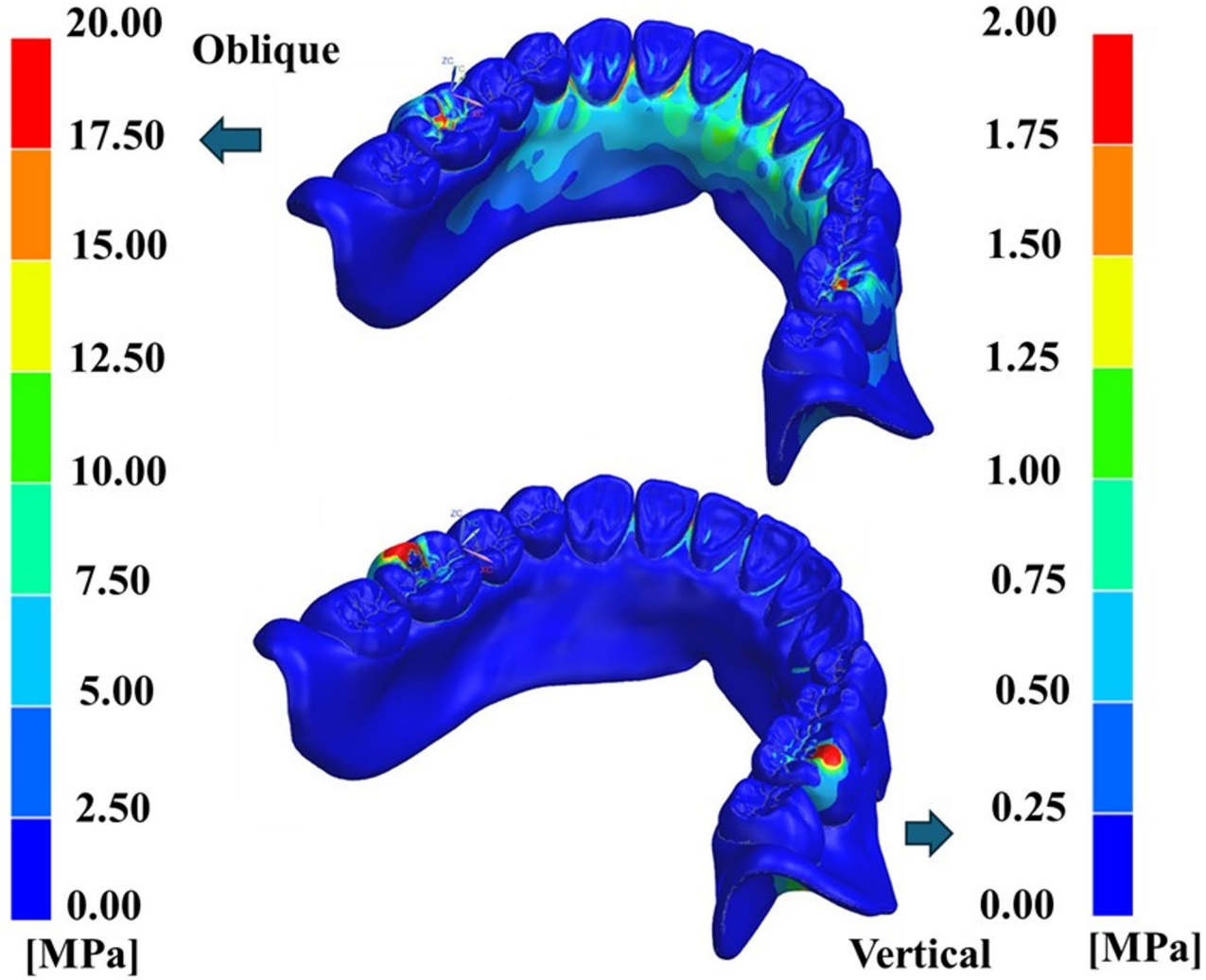

Fig. 6. Maximum principal nodal stress (tension) value under bilateral oblique 140 N forces and vertical 100 N.

stresses capable of explaining the most frequent clinical fractures in the anterior zone. In the case of local stress concentration, a higher stress value of 29 MPa was observed at the transition between the molar and premolar teeth, while 25 MPa was observed for the canine tooth.

Here, it is necessary to distinguish between immediate fractures and fatigue fractures. The mechanism of fatigue fracture depends on the number and amplitude of cycles and material degradation, and the value of the cyclic load results from food comminution, which requires much lower values than the maximum occlusal force. Immediate fractures should be related to the maximum occlusal forces and instantaneous strength, while lower values of cyclic forces should be related to fatigue strength.

The ultimate flexural strength of PMMA denture base materials is governed by ISO 20795-1:2013 (Dentistry - Base Polymers - Part 1: Denture Base Polymers), which specifies a minimum flexural strength of 65 MPa for heat-polymerized PMMA. Commercially available PMMA materials typically exhibit ultimate flexural strengths ranging from 70 to 90 MPa, with values often clustering around 80 MPa under standardized three-point bending tests[21]. However, there are examples of strength reaching 130-146MPa[22–24]. The critical stress area in the anterior segment should be referred to tensile strength. Tensile strength studies are not as popular, however, denture base materials typically range from 40 to 120 MPa, depending on processing techniques such as heat polymerization, injection molding, or CAD-CAM milling[25–34]. Brittle PMMAs generally exhibit around 1.5–2 times higher compressive strength than tensile strength. This suggests that the use of hydrostatic-dependent criteria may better capture failure. Drucker-Prager or parabolic modifications (e.g., Raghava-type) of Mohr-Coulomb would predict higher allowable stresses in compressive or mixed zones compared to eqvHMH stress, thereby further reducing the estimated failure risk in posterior regions where stresses originate from compressive nature. Similarly, in mixed tension-compression zones. However, in the state of biaxial tension, caution should be exercised when applying the eqvHMH criterion, which may overestimate strength (i.e., underestimate failure risk). It is safer to use the principal stress criterion. We did not observe a dangerous state in this criterion, as the observed stresses represent a mixed state far from equibiaxial tension (biaxiality ratio 0.5–0.6.). The Drucker-

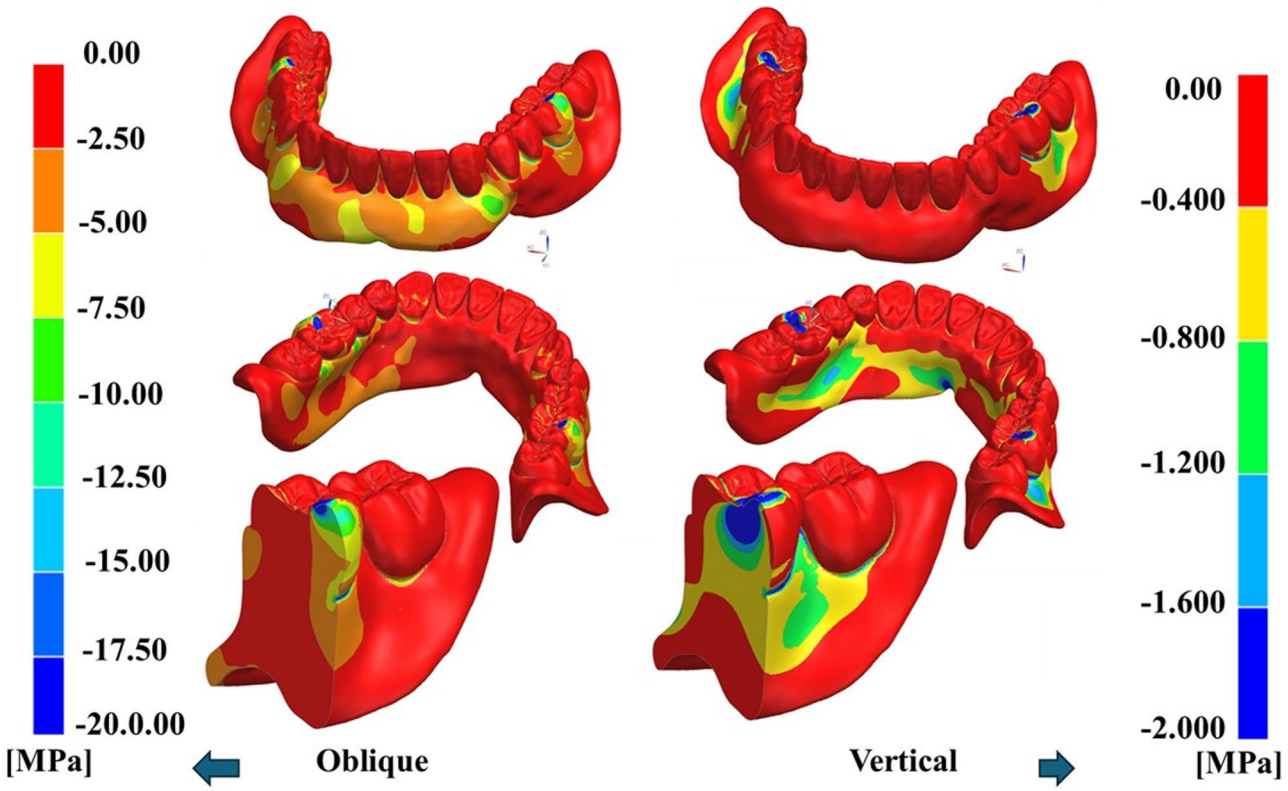

Fig. 7. Minimum principal nodal stress (compression) value under bilateral oblique 140 N forces and vertical 100 N.

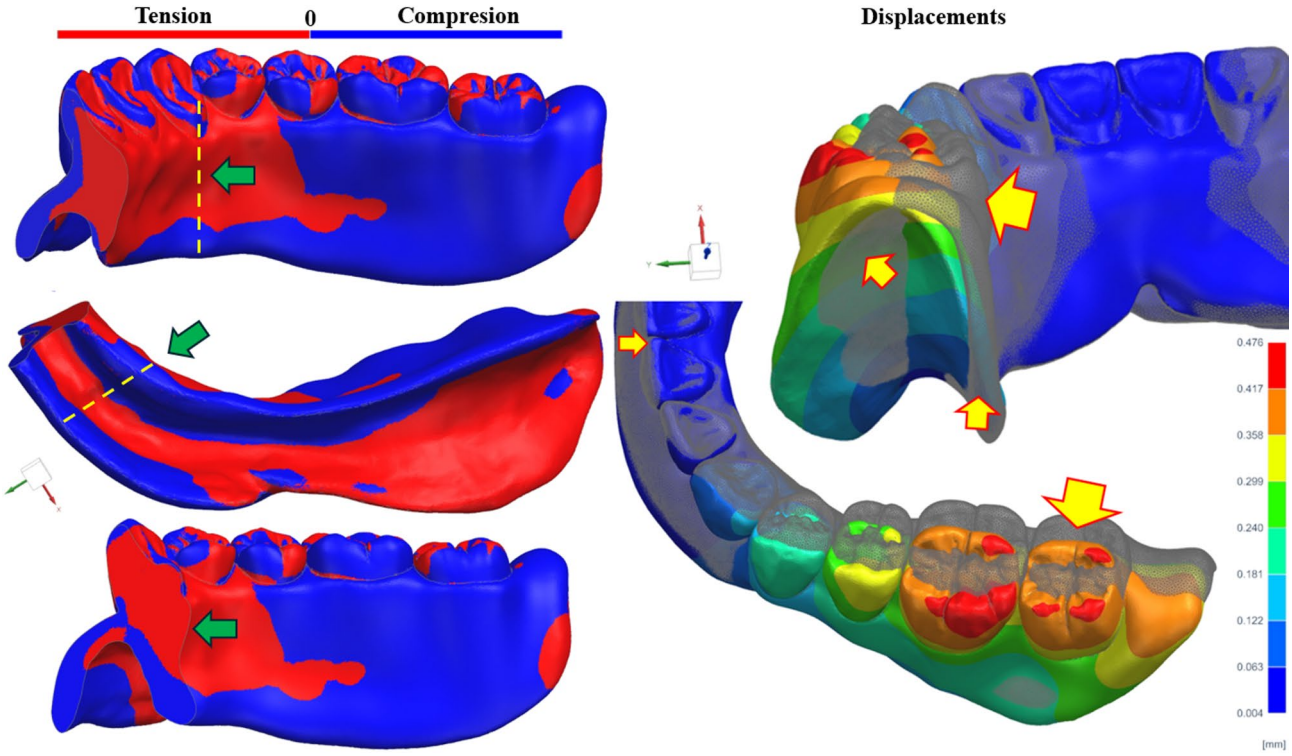

Fig. 8. Maximum and minimum principal stress revealing tension and compression in a cross-section centrally through the incisors and through the canine (green guide) and displacements (scaled 4:1) with directional indications relative to the undeformed model. Bilateral oblique mastication force 140 N.

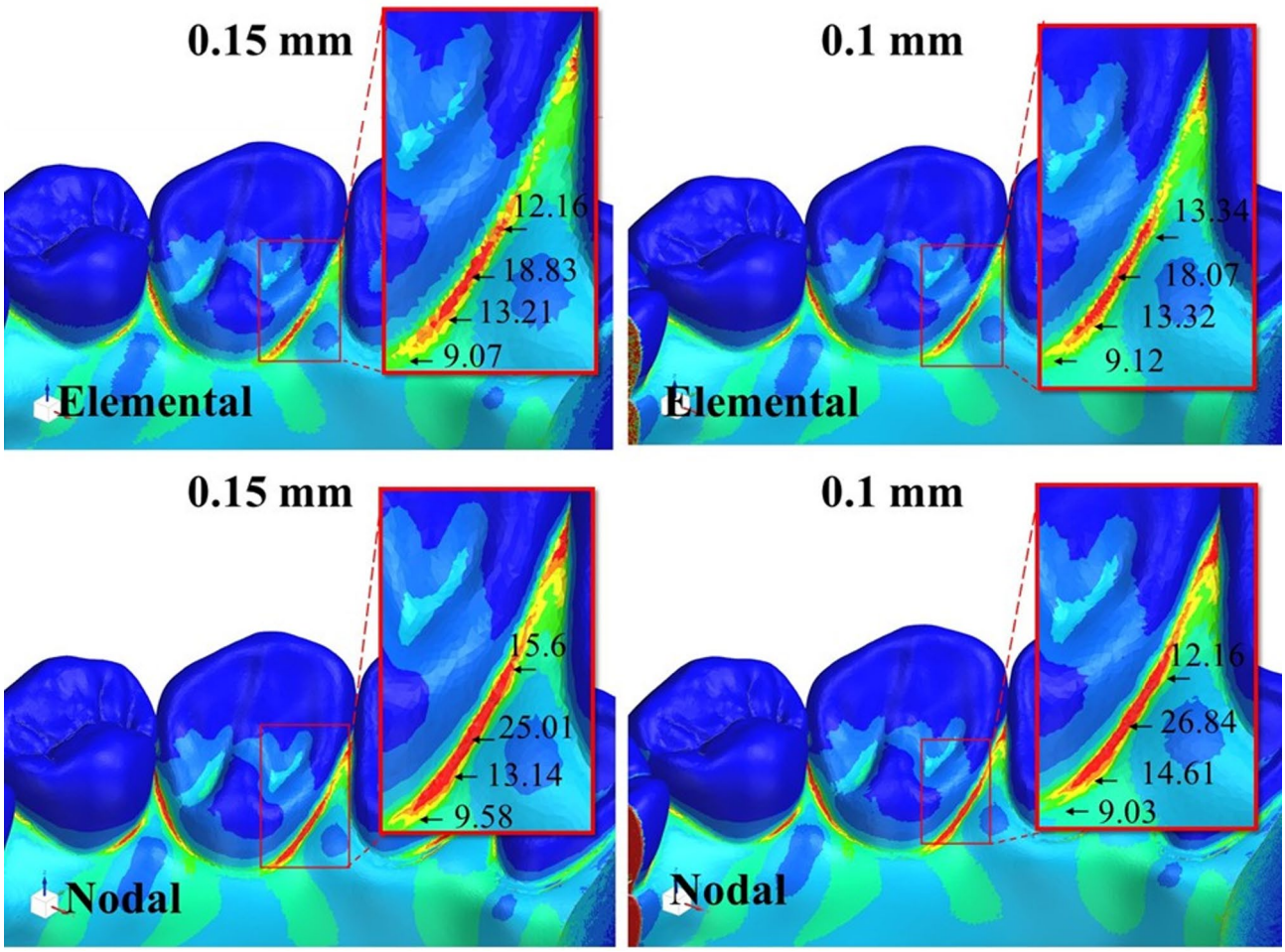

Fig. 9. Elemental and nodal equivalent Huber-Mises-Hencky stress values after local mesh size increments to 0.15 mm and 0.1 mm on the zone between the canine and incisor. Bilateral oblique 140 N forces.

Prager criterion is even more conservative in states of near-equibiaxial tension. There are several examples. In the study[35], in equibiaxial tension yield stress for PMMA was approximately 40–50 MPa, while eqvHMH stress predicted 55–70 MPa (20–40% overestimation). Similarly, in[36], in biaxial tension for PMMA measured values were lower than predicted by eqvHMH (45 MPa vs. 55 MPa, 15–25% lower). The work[37] also indicates that eqvHMH overestimates by 20–30% in biaxial paths (~ 50 MPa measured vs. ~ 60–65 MPa predicted). Even assuming a conservative tensile strength of 40–50 MPa, the stresses in our model remain significantly lower (with approximately 3-fold safety margin at 140 N).

However, such conservative criteria appear to excessively underestimate the strength of current modern denture materials. Firstly, the state was far from biaxial uniform tension. Secondly, there are available results of studies on the biaxial states of brittle polymers dating back many years[35–37]. Denture base materials have evolved from simple brittle PMMA and, through modifying additives, have achieved significant elongation at break of up to 2–6%[25–30,32,34,38,39], or even 10–30%, depending on the injection or printing technology used[40–42]. In light of this, it appears that adopting a conservative criterion for currently used denture materials excessively underestimates their strength in the equibiaxial state (i.e., overestimates failure risk). However, this remains speculative due to the lack of biaxial/multiaxial data for current PMMA denture resins.

In the model, we assumed a bite force load of 140 N, which could be negated as too low. It is clinically documented that in the case of implant-fixed dentures[43] full bite forces can be recovered. The chewing forces, which should be related to fatigue strength, reach standard values of 250–350 N, as in people with full natural dentition. Maximum bite forces, which should be related to immediate strength, are also recovered significantly above 500 N, corresponding to nominal mandibular muscle forces[44].

Bite forces in removable complete denture wearers are constrained by mucosal and bone support, denture instability, and pain. It is well documented clinically that full bite force recovery is not achieved with traditional dentures and is significantly lower compared to implant-fixed dentures and two-implant retained soft tissue-supported removable dentures. The bite force is 139 N for a removable complete denture and almost twice as high at 235 N for a two-implant-supported removable prosthesis in work[45]. Also in[46] bite forces for removable dentures are twice as low as for overdentures on two implants. Similarly, in[47] the force for removable dentures is 254 N and 416 N for overdentures and even 841 N for 8-implant fixed dentures. Studies report bite forces in

removable complete denture wearers typically ranging from 35 to 200 N in the posterior region[48–50]. However, removable denture wearers can, in exceptional cases, achieve surprisingly high values, reaching 461 N[51] and even exceeding 500 N[52]. If we apply these individual cases of denture wearers to our model, then assuming a linear increase from 140 N to 500 N, we would have a 3.57x higher stress of 35–70 MPa. These values begin to approach the tensile strength of denture materials. However, even if we assume that these few cases of denture wearers with bite force values of about 500 N justify fractures, the statistics small number of such denture wearers[51,52] is inconsistent with a significant number of fractures.

In work[53] stress reaches of 10.9–12.2 MPa under vertical load of 100 N, however it is peak value at artifact node at force application. The value 7.8 MPa is also artifact because at edge between tooth and base and in more distant zones value about 3 MPa is visible. The model is rigidly supported on a metal base, which is not able to deform like a resilient mucosal foundation. In such conditions, the material is mainly subjected to stress generated by local pressing against the foundation. Mucosal resiliency is considered in[16], and the load force was 100 N and vertically oriented. Mesh is smooth and elements are relatively lower in size. However, only the posterior part of dentures is modeled in limitation to molars zone.

In the work[11] tensile strain reaches values of only 0.18–0.19%, which at modulus of elasticity 3200 MPa gives stresses of 6.4 MPa far from critical. Compression strain reaches 0.36% only around labial frenal notch, which is still far from critical values. The model was loaded with two symmetrical vertical occlusal forces on molars of 230 N each and the model contained 256,431 tetrahedral elements and their size was smaller compared to the work[54]. In work[55] the size of finite elements of 0.5 mm on the surface of the prosthesis was assumed as appropriate and the number of elements in the model was 61,108. The optimization of the prosthesis reinforcement design was based on the displacement of the prosthesis, which was rigidly supported on the mucosa. This makes it difficult to compare the results, as the dentures work on an flexible foundation, which significantly changes their deformation mechanism. Nevertheless, the results of our work, as well as the convergence analysis in[55] confirm that the optimization approach requires taking into account the stress criterion. Also in[55] with increasing the number of elements, higher stresses were obtained, although the displacements were considered convergent. The values of maximal principal stress for the mesh of 2, 1, 0.5 and 0.25 mm were 20.7, 20.7, 24.5 MPa and 34.8 MPa, respectively. Unfortunately, the stress distribution was not shown in the work[55], so it is not known in which area these values occurred. It is known, however, that vertical forces were applied simultaneously with values of 900 N on posterior teeth, 450 N on premolars and 150 N on anterior teeth. The stresses were much lower than the critical ones for denture materials, although these forces were much higher than those recorded for removable denture wearers and natural dentition.

Difficulties in explaining fractures lead to the search for reasons in material fatigue and the processes of crack initiation and growth. In fatigue analysis, it is important to determine the number of cycles and the average value of loads during mastication. Removable denture wearers perform approximately 2,000–7,500 chewing cycles per day, with a median of 4,000–5,000 cycles, based on 20–50 cycles per bite and 100–150 bites daily, as derived from studies on mastication efficiency[56–60]. Assuming an average of 5,000 cycles per day, 1 million cycles would be reached in approximately 200 days (1,000,000 ÷ 5,000 = 200 days), or roughly 6.5 months of continuous use. For a lower estimate of 2,000 cycles/day, this extends to 500 days (1.5 years), and for an upper estimate of 7,500 cycles/day, it reduces to 133 days (4.5 months).

In the work[13] it is suggested that defects increase stress around crack to value 112 MPa. However, it was not stated what force was used to load the denture. Besides, the stress value in node at crack tip in FEM is singular point and artifact. Determining the exact value in artifact node requires a special procedure to assess the effect of mesh size and approximation or extrapolation from nodes adjacent to the singular node. It is therefore not known how to relate the results of the work[13] to the singular node, however it seems that the stress was at least twice as small in the areas distant from the node bordering the defect. More information can be found in another work of this team[54], which states that the upper denture was loaded with 70 N vertically and symmetrically. The denture model consisted of 154,742 tetrahedral elements, which is similar in size to our initial model. The approach to cracking by assuming a void is original and presents an interesting modeling technique, however, in practice, in a well-made prosthesis, the voids are the same size as in the samples on which fatigue strength is tested. The crack assumed in work[54] is substantially larger than typical voids in fatigue-tested denture materials (10–200 µm)[61–63]. These cracks are 5–100 times larger than common voids, suggesting they are oversized relative to typical porosity. The studies appear to model worst-case scenarios, simulating macroscopic flaws (for example from a denture impact) rather than microscopic voids, which may not fully represent the defect population in well-processed denture materials. The fatigue strength value tested on the samples includes such typical imperfections as well as the effects of aging and residual monomer washout[64]. Therefore, these values of stress calculated by simulation can be directly related to fatigue strength without introducing defects in the material.

Our results show that local fillet radii introduced stress values in the range decisive for fatigue life. In our analysis, stresses in the canine zone were exactly in the fatigue strength range (10–20 MPa). However, it is clear that by slightly increasing the fillet, it would be easy to achieve a stress reduction below 10 MPa, so the fatigue strength limit has not been reached even for the weakest materials. The value of the force accompanying mastication is not certain. According to sources, the value 140 N we have adopted is in the upper range and maximal force while about half of the value is considered as necessary for food comminution and mastication[48–50,65–70]. Some studies may suggest that forces accompanying mastication may reach 200–250 N[48,51,52], but these are maximum forces and individual cases as we discussed earlier.

Compression fatigue strength at 1 Hz is higher than tensile or flexural strength and ranges between 34-40MPa[71], which could justify the hypothesis that if the lateral segment is compressed, lower tensile fatigue strength justifies the occurrence of fracture earlier in the anterior segment than in the posterior segment. On the other hand, our results indicate that the denture was bent in the critical anterior region, so bending tests on specimens in which one side works in tension and the other in compression (labial/lingual) are reliable in terms

of fatigue strength. We also took over the good conditions of the alveolar ridge, which favour higher mastication forces[48,65,69,72], and also, by limiting the available space, force thinner and less durable prostheses.

Some studies indicate that material fatigue is not necessary for fracture. In a large research group in[73] out of 22.4% of all fractures most of them occurred from 6 months to 1 year after insertion. Similarly in[74] out of 160 fractures 16% occurred in the initial period of 6 months and 38% in 6–12 months and 45% in the period of 12–36 months. Studies of the morphology of fractures that occurred in oral cavity during service are limited and we find basically only one work[75] from 50 years ago on 7 dentures. The fracture topography of acrylic complete dentures reveals[75] fine, regular striations, smooth surfaces indicative of slow crack growth, and rough terminal zones, suggesting a possible mixed fracture mechanism, though mastication as a cause remains unconfirmed. Differences in striation size and regularity and hackle mark prominence remain unclear due to limited clinical context in[75]. The works[76–78] are helpful in distinguishing the type of fracture in samples, in which the main differences are indicated. Presence of regular striations (1–10 μm spacing) is diagnostic, indicating cyclic loading. Fatigue zones dominate (50–70%), with smooth areas and minimal hackle marks. Impact fracture is characterized with chaotic river lines (10–50 μm), prominent hackle marks, and rough, fragmented terminal zones and no striations. Static fracture shows straighter river lines (10–30 μm), subtle hackle marks, cleavage steps, less rough terminal zones and no striations. In practice, the distinction between striations and river lines leaves much room for interpretation, especially since, as we have shown in our calculations, fracture initiation and its course may occur from several stress concentration areas simultaneously, i.e. in a completely different way than in samples with full knowledge and control of the fracture initiation area and knowledge of the loading history.

Our results indicated that stress concentration around small interdental and cervical grooves should be addressed in the prevention of fatigue fractures, a topic that is largely absent in the current state of knowledge. Beyond studies focusing on exaggerated undercuts or defects to induce fracture conditions[13,14], such as large voids or frenum notches, there has been no detailed analysis of anatomical grooves with radii below 0.3–0.8 mm on strength of removable dentures. The main limitation of our analysis was the use of elements no smaller than 0.3 mm. As is known, any curvatures on anatomical shapes smaller than the size of finite elements are ignored in the FEM model, because the mesh generator approximates the shapes to the assumed size of finite elements. The observed convergence (elemental-nodal stress difference ≤ 10%) suggests that the 0.3 mm mesh is sufficient for study purposes, but local refinement could enhance accuracy in future studies targeting the smallest anatomical features. The choice of a 0.3 mm mesh size in this study was guided by the need to maintain computational efficiency and taking into account critical anatomical features. Cervical margins and interdental grooves exhibit fillet radii of 0.1–0.5 mm and 0.2–0.8 mm, respectively[8,79,80]. The 0.3 mm parabolic 10-node element size is centrally positioned within these ranges, but ensuring adequate resolution for higher radii value about 0.6 mm, because minimum 4 elements at the bottom of the groove are required. It points out that the areas most stressed by tension are located on the lingual side. Aesthetics are not required there. Also, the canine area, which is one of the most heavily loaded, is not very visible during a smile, especially in the lower denture. It seems better to design these areas with a certain disregard for aesthetics. Our results may be useful for dental technicians in designing, as they schematically show red areas, the smooth filling of which allows to avoid stresses close to fatigue strength.

To address fractures, dental technicians should prioritize smoothing these red areas and maximizing radii to the upper range of 0.5–0.8 mm given in prosthetics, and in the case of stable conditions of a convex foundation and a thin denture saddle, it is best to fill the interdental space on the lingual side as tangentially as possible to the saddle and tooth surfaces. However, further studies are needed to obtain precise data for designing which fillet radii are critical and pose a risk of fracture as a result of local stress concentration. Without further analysis, it is difficult to say whether it is possible to reduce stress and achieve fatigue life thanks to fillets while maintaining acceptable aesthetics under such load. Currently, despite the fact that the use of dentures reaches 100 years, we lack data. This is due to the fact that clinical fracture data do not measure and classify the basic geometric parameters necessary to assess fatigue life. The shapes of these local details depend on the manufacturing technology used. In traditional dentures, the technician can easily eliminate excessively sharp transitions between teeth by waxing the teeth. In CAD/CAM dentures, gluing teeth requires an oversized hole in the denture base for the adhesive bond. The design process for dentures for CAM differs from that for aimed for FEA, which requires no gaps for adhesive bonding. Obtaining the same shape as with adhesive bonding is challenging and may require separate future work. In principle, it would be necessary to scan several finished dentures and compare them to the CAD model. A strategy for designing denture models for FEA analysis would be developed, especially if one wants to study cervical margins and interdental grooves depending on radius size.

The limitation of our model was also the linear behaviour of the mucosa. On the other hand, the stresses in the prosthesis are influenced by the final deflection of the prosthesis on the flexible soft tissue, while the nonlinear hyperelastic behaviour can be approximated by a single modulus of elasticity. The secant modulus value for the mucosa, depending on the points for higher loads in the range of 100–300 kPa, takes values between 0.4 and 1 MPa[1,81]. In the work[1], although 3,188,247 elements were used, the model contained whole mandible and implant retained dentures, and the work was focused on soft tissue loads, so the load capacity of denture results cannot be compared. There are many works[82–85] concerning the loading of soft mucosa and bone tissue beneath dentures, including implant-retained overdentures, but in such works the denture load bearing capacity is not analysed. In addition, this type of prosthesis breaks in the area of the action of the supporting forces on the implants[86], where additionally the cross-section of the prosthesis is reduced by the cavity for the implant attachment. However, it is noted that the modulus of elasticity of the foundation based on the work[81] does not take into account the fact that the characteristic of the mucosa under the prosthesis is stiffer compared to the characteristic under the penetrator[19]. The reason is the limitation of deformation by the denture saddle.

Therefore, smaller moduli of elasticity based on the penetration characteristic do not seem to correspond to the conditions of compression under denture saddle.

Despite constraints from the denture saddle, the mucosa exhibits patient-specific and local variability in deformation and viscoelastic behavior[87]. Increased deformation due to tissue compliance and creep reduces stresses in the mucosa by 20–50% through creep-induced relaxation[1,88,89]. Load redistribution occurs from highly compressed posterior regions to less loaded anterior ones. Consequently, reaction forces under the denture wings may shift forward, which increases outward bending of the denture arch. Higher mucosal compliance elevates denture base stresses by up to 30%[89,90]. However, studies using 2D models or different loading conditions may distort actual effects. The extent to which creep influences critical stresses, particularly under destabilized conditions (e.g., asymmetric support amplifying bending), remains for future investigation.

The third limitation was the perfect fit and adhesion of the denture to the mucosa, which in real conditions slips and detaches from the mucosa.

Conclusions

1. Vertical forces generated stress values incomparably lower than the material strength, and only oblique forces should be considered as relevant for potential failure.
2. Under oblique bilateral mastication forces typical of denture wearers, the anterior zone exhibited nominal stresses originating from tension on the lingual side and compression on the labial side. These values were significantly lower than the material's tensile strength, even in tension-dominant zones under conservative criteria for semi-brittle polymer. This negated the hypothesis that denture fracture in the anterior segment is possible under such conditions.
3. The study also showed that, under the commonly assumed loading scheme, the stress in properly manufactured dentures without defects or excessive grooves does not reach the fatigue strength of the denture materials. The prevailing view regarding the fatigue fracture mechanism relies on limited historical fractographic analyses of only a few in-service failures and therefore requires further validation through comprehensive fractographic studies of dentures fractured in the oral cavity.
4. Further investigation is required, incorporating factors such as denture foundation resiliency, misfit, occlusal imbalance, and potentially different loading patterns to fully elucidate intraoral failure modes.

Data availability

The datasets used and/or analysed during the current study available from the corresponding author on reasonable request.

Received: 5 August 2025; Accepted: 24 January 2026
Published online: 04 March 2026

References

1. Chen, J., Ahmad, R., Li, W., Swain, M. & Li, Q. Biomechanics of oral mucosa. *J. R Soc. Interface.* **12**, 20150325. https://doi.org/10.1098/rsif.2015.0325 (2015).
2. Im, S. M., Huh, Y. H., Cho, L. R. & Park, C. J. Comparison of the fracture resistances of glass fiber Mesh- and metal Mesh-Reinforced maxillary complete denture under dynamic fatigue loading. *J. Adv. Prosthodont.* **9**, 22–30. https://doi.org/10.4047/jap.2017.9.1.22 (2017).
3. Darbar, U. R., Huggett, R. & Harrison, A. Denture Fracture–a survey. *Br. Dent. J.* **176**, 342–345. https://doi.org/10.1038/sj.bdj.4808449 (1994).
4. Bosânceanu, D. N. et al. COMPLETE DENTURES FRACTURES –CAUSES AND INCIDENCE. *9*, 54–59. (2017).
5. Bhattacharya, S. R., Ray, P. K., Makhal, M. & Sen, S. K. INCIDENCE AND CAUSES OF FRACTURE OF ACRYLIC RESIN COMPLETE DENTURE. *Jemds* **3**, 14787–14793. https://doi.org/10.14260/Jemds/2014/3986 (2014).
6. Yu, S. H., Oh, S., Cho, H. W. & Bae, J. M. Reinforcing effect of Glass-Fiber mesh on complete dentures in a test model with a simulated oral mucosa. *J. Prosthet. Dent.* **118**, 650–657. https://doi.org/10.1016/j.prosdent.2017.03.018 (2017).
7. Takahashi, Y., Yoshida, K. & Shimizu, H. Effect of location of glass Fiber-Reinforced composite reinforcement on the flexural properties of a maxillary complete denture in vitro. *Acta Odontol. Scand.* **69**, 215–221. https://doi.org/10.3109/00016357.2010.549506 (2011).
8. Prosthodontic Treatment for Edentulous Patients - Edition 13 -, By George, A. & Zarb BchD(Malta), DDS, MS(Michigan), FRCD(Canada), John Hobkirk, Steven Eckert, DDS, MS and Rhonda Jacob, BS, MS, DDSElsevier Health Inspection Copies Available online: https://www.inspectioncopy.elsevier.com/book/details/9780323078443 (accessed on 17 April 2025).
9. Miyashita, K. et al. Denture mobility with six degrees of freedom during function. *J. Oral Rehabil.* **25**, 545–552. https://doi.org/10.1046/j.1365-2842.1998.00273.x (1998).
10. Chong, L. C. Movement of maxillary complete Dentures–a kinesiographic study. *J. Dent.* **11**, 257–263. https://doi.org/10.1016/0300-5712(83)90198-7 (1983).
11. Cheng, Y. Y., Cheung, W. L. & Chow, T. W. Strain analysis of maxillary complete denture with Three-Dimensional finite element method. *J. Prosthet. Dent.* **103**, 309–318. https://doi.org/10.1016/S0022-3913(10)60064-9 (2010).
12. Nejatidanesh, F., Peimannia, E. & Savabi, O. Effect of labial frenum Notch size and palatal vault depth on stress concentration in a maxillary complete denture: A finite element study. *J. Contemp. Dent. Pract.* **10**, 59–66 (2009).
13. Cernescu, A. et al. Reverse Engineering and FEM Analysis for Mechanical Strength Evaluation of Complete Dentures: A Case Study. In *Reverse Engineering - Recent Advances and Applications*; IntechOpen, ISBN 978-953-51-0158-1. (2012).
14. Lee, J. H. et al. A finite element analysis study of edentulous model with complete denture to simulate masticatory movement. *Bioengineering* **11**, 336. https://doi.org/10.3390/bioengineering11040336 (2024).
15. Grachev, D. I. et al. Algorithm for designing a removable complete denture (RCD) based on the FEM analysis of its service life. *Mater. (Basel).* **15**, 7246. https://doi.org/10.3390/ma15207246 (2022).
16. Mankani, N., Chowdhary, R. & Mahoorkar, S. Comparison of stress dissipation pattern underneath complete denture with various posterior teeth form: an in vitro study. *J. Indian Prosthodont. Soc.* **13**, 212–219. https://doi.org/10.1007/s13191-012-0193-y (2013).

17. Takayama, Y., Yamada, T., Araki, O., Seki, T. & Kawasaki, T. The dynamic behaviour of a lower complete denture during unilateral loads: analysis using the finite element method. *J. Oral Rehabil.* **28**, 1064–1074. https://doi.org/10.1046/j.1365-2842.2001.00759.x (2001).
18. Wakabayashi, N. Patient-Specific Finite Element Analysis of Viscoelastic Masticatory Mucosa.
19. Żmudzki, J., Chladek, G. & Kasperski, J. Biomechanical factors related to occlusal load transfer in removable complete dentures. *Biomech. Model. Mechanobiol.* **14**, 679–691. https://doi.org/10.1007/s10237-014-0642-0 (2015).
20. Marcián, P. et al. On the limits of finite element models created from (Micro)CT datasets and used in studies of Bone-Implant-Related Biomechanical problems. *J. Mech. Behav. Biomed. Mater.* **117**, 104393. https://doi.org/10.1016/j.jmbbm.2021.104393 (2021).
21. Chhabra, M., Nanditha Kumar, M., RaghavendraSwamy, K. N. & Thippeswamy, H. M. Flexural strength and impact strength of Heat-Cured acrylic and 3D printed denture base Resins- A comparative in vitro study. *J. Oral Biol. Craniofac. Res.* **12**, 1–3. https://doi.org/10.1016/j.jobcr.2021.09.018 (2022).
22. Takaichi, A. et al. Systematic review of digital removable partial dentures. Part II: CAD/CAM Framework, artificial Teeth, and denture base. *J. Prosthodontic Res.* **66**, 53–67. https://doi.org/10.2186/jpr.JPR_D_20_00117 (2022).
23. Barbosa, D. B., Souza, R. F. & de Flexural strength of acrylic resins polymerized by different cycles. *J. Appl. Oral Sci.* **15**, 424–428. https://doi.org/10.1590/S1678-77572007000500010 (2007). PeroA.C.Marra, J.; Compagnoni, M.A.
24. Chladek, G. et al. Effect of antibacterial Silver-Releasing filler on the physicochemical properties of Poly(Methyl Methacrylate) denture base material. *Mater. (Basel).* **12**, 4146. https://doi.org/10.3390/ma12244146 (2019).
25. Spasojević, P. et al. Poly(Methyl Methacrylate) denture base materials modified with Ditetrahydrofurfuryl itaconate: significant applicative properties. *J. Serb. Chem. Soc.* **80**, 1177–1192. https://doi.org/10.2298/JSC150123034S (2015).
26. Oleiwi, J. K. & Hamad, Q. A. Studying the mechanical properties of denture base materials fabricated from polymer composite materials. *Al-Khwarizmi Eng. J.* **14**, 100–111. https://doi.org/10.22153/kej.2018.01.006 (2018).
27. Demir, H., Dogan, O. M. & Dogan, A. Tensile properties of denture base resin reinforced with various esthetic fibers. *J. Appl. Polym. Sci.* **123**, 3354–3362. https://doi.org/10.1002/app.33831 (2012).
28. Doğan, A., Bek, B., Çevik, N. N. & Usanmaz, A. The effect of Preparation conditions of acrylic denture base materials on the level of residual Monomer, mechanical properties and water absorption. *J. Dent.* **23**, 313–318. https://doi.org/10.1016/0300-5712(94)00002-W (1995).
29. R, S. A. et al. Comparative analysis of strength of differently activated denture base materials including recent acetal Resin-Based Biodentaplast. *Cureus* **16** https://doi.org/10.7759/cureus.54676 (2024).
30. Bortun, C. M. et al. Structural investigation concerning mechanical behaviour of two dental acrylic resins. *Materiale Plastice* **45** 362–365. (2008).
31. Al-Ameri, A. et al. An In-Vitro evaluation of Strength, Hardness, and color stability of Heat-Polymerized and 3D-Printed denture base polymers after aging. *Polymers* **17** https://doi.org/10.3390/polym17030288 (2025).
32. Barbur, I. et al. Statistical comparison of the mechanical properties of 3D-Printed resin through Triple-Jetting technology and conventional PMMA in orthodontic occlusal splint manufacturing. *Biomedicines* **11** https://doi.org/10.3390/biomedicines11082155 (2023).
33. Chuchulska, B. & Zlatev, S. Linear dimensional change and ultimate tensile strength of polyamide materials for denture bases. *Polym. (Basel).* **13**, 3446. https://doi.org/10.3390/polym13193446 (2021).
34. Takabayashi, Y. Characteristics of denture thermoplastic resins for Non-Metal clasp dentures. *Dent. Mater. J.* **29**, 353–361. https://doi.org/10.4012/dmj.2009-114 (2010).
35. Raghava, R., Caddell, R. M. & Yeh, G. S. Y. The macroscopic yield behaviour of polymers. *J. Mater. Sci.* **8**, 225–232. https://doi.org/10.1007/BF00550671 (1973).
36. Sternstein S. andOngchin L.,Yield Criteria for Plastic Deforation of Glassy High Polymers in General Stress Fields, *A.C.S. Polymer Rep.* **10**(2), 1117–1124 (1969).
37. Pae, K. D. The macroscopic yielding behaviour of polymers in multiaxial stress fields. *J. Mater. Sci.* **12**, 1209–1214. https://doi.org/10.1007/BF02426859 (1977).
38. Vallittu, P. k. The Effect of Void Space and Polymerization Time on Transverse Strength of Acrylic-Glass Fibre Composite. *Journal of Oral Rehabilitation 22*, 257–261, (1995). https://doi.org/10.1111/j.1365-2842.1995.tb00083.x
39. Chhabra, M., Nanditha Kumar, M., RaghavendraSwamy, K. N. & Thippeswamy, H. M. Flexural strength and impact strength of Heat-Cured acrylic and 3D printed denture base Resins- A comparative in vitro study. *J. Oral Biology Craniofac. Res.* **12**, 1–3. https://doi.org/10.1016/j.jobcr.2021.09.018 (2022).
40. Aura3D Aura3D Available online. January (2026). https://aura3d.us/dental-resin (accessed on 3.
41. Lee, J. M. et al. Optimizing printing temperature and Post-Curing time for enhanced mechanical property and fabrication reproducibility of 3D-Printed dental photopolymer resins. *Appl. Sci.* **15** https://doi.org/10.3390/app152111552 (2025).
42. Catalog - HARZ Labs Available online. January (2026). https://harzlabs.com/products/materialy/dental-denture-base.html (accessed on 2.
43. Thomková, B., Marcián, P., Borák, L., Joukal, M. & Wolff, J. Biomechanical performance of dental implants inserted in different mandible locations and at different angles: A finite element study. *J. Prosthet. Dent.* **131**, 128e1. 128.e10 (2024).
44. AL-Omiri, M. K. et al. Maximum bite force following unilateral Implant-Supported prosthetic treatment: Within-Subject comparison to opposite dentate side. *J. Rehabil.* **41**, 624–629. https://doi.org/10.1111/joor.12174 (2014).
45. Fontijn-Tekamp, F. A., Slagter, A. P., van't Hof, M. A., Geertman, M. E. & Kalk, W. Bite forces with mandibular Implant-Retained overdentures. *J. Dent. Res.* **77**, 1832–1839. https://doi.org/10.1177/00220345980770101101 (1998).
46. Rismanchian, M., Bajoghli, F., Mostajeran, Z., Fazel, A. & Eshkevari, P. Effect of implants on maximum bite force in edentulous patients. *J. Oral Implantology*. **35**, 196–200. https://doi.org/10.1563/1548-1336-35.4.196 (2009).
47. Baca, E., Yengin, E., Gökçen-Röhlig, B. & Sato, S. In vivo evaluation of occlusalcontact area and maximum bite force in patients with various types of Implant-Supported prostheses. *Acta Odontol. Scand.* **71**, 1181–1187. https://doi.org/10.3109/00016357.2012.757360 (2013).
48. Müller, F., Heath, M. R. & Ott, R. Maximum bite force after the replacement of complete dentures. *Gerodontology* **18**, 58–62. https://doi.org/10.1111/j.1741-2358.2001.00058.x (2001).
49. Fontijn-Tekamp, F. A. et al. Biting and chewing in Overdentures, full Dentures, and natural dentitions. *J. Dent. Res.* **79**, 1519–1524. https://doi.org/10.1177/00220345000790071501 (2000).
50. (PDF) Bite Force Evaluation in Complete Denture Wearer with Different Denture Base Materials: A Randomized Controlled Clinical Trial. ResearchGate. (2024). https://doi.org/10.4103/jispcd.JISPCD_2_18
51. Shala, K. et al. Evaluation of maximum bite force in patients with complete dentures. *Open. Access. Maced J. Med. Sci.* **6**, 559–563. https://doi.org/10.3889/oamjms.2018.141 (2018).
52. Lee, J. H., Kim, W. H., Shin, R. H. & Lee, K. W. A comparison of the masticatory function between two different types of implant supported prostheses and complete denture for fully edentulous patients. *J. Korean Acad. Prosthodont.* **46**, 591. https://doi.org/10.4047/jkap.2008.46.6.591 (2008).
53. Grachev, D. I. et al. Ranking technologies of additive manufacturing of removable complete dentures by the results of their mechanical testing. *Dentistry J.* **11**, 265. https://doi.org/10.3390/dj11110265 (2023).
54. Cernescu, A., Faur, N., Bortun, C. & Hluscu, M. A. Methodology for fracture strength evaluation of complete denture. *Eng. Fail. Anal.* **18**, 1253–1261. https://doi.org/10.1016/j.engfailanal.2011.03.004 (2011).

55. Altunay, R. et al. Denture reinforcement via topology optimization. *Medical Engineering Physics*. **135**, 104272. https://doi.org/10.1016/j.medengphy.2024.104272 (2025).
56. Jemt, T. Chewing patterns in dentate and complete denture Wearers - Recorded by Light-Emitting diodes. *Swed. Dent. J.* **5**, 199–205 (1981).
57. Kohyama, K., Mioche, L. & Martin, J. F. Chewing patterns of various texture foods studied by electromyography in young and elderly populations. *J. Texture Stud.* **33**, 269–283. https://doi.org/10.1111/j.1745-4603.2002.tb01349.x (2002).
58. Grigoriadis, A., Johansson, R. S. & Trulsson, M. Adaptability of mastication in people with Implant-Supported bridges. *J. Clin. Periodontol.* **38**, 395–404. https://doi.org/10.1111/j.1600-051X.2010.01697.x (2011).
59. Mishellany-Dutour, A., Renaud, J., Peyron, M. A., Rimek, F. & Woda, A. Is the goal of mastication reached in young dentates, aged dentates and aged denture wearers? *Br. J. Nutr.* **99**, 121–128. https://doi.org/10.1017/S0007114507795284 (2008).
60. Postić, S. D., Krstić, M. S. & Teodosijević, M. V. A comparative study of the chewing cycles of dentate and Denture-Wearing subjects. *Int. J. Prosthodont.* **5**, 244–256 (1992).
61. Chladek, G., Adeeb, S., Pakieła, W. & Coto, N. P. Effect of different surface treatments as methods of improving the mechanical properties after repairs of PMMA for dentures. *Mater. (Basel)*. **17**, 3254. https://doi.org/10.3390/ma17133254 (2024).
62. Vallittu, P. K. The effect of void space and polymerization time on transverse strength of Acrylic-Glass fibre composite. *J. Oral Rehabil.* **22**, 257–261. https://doi.org/10.1111/j.1365-2842.1995.tb00083.x (1995).
63. Becerra, J., Mainjot, A., Hüe, O., Sadoun, M. & Nguyen, J. F. Influence of High-Pressure polymerization on mechanical properties of denture base resins. *J. Prosthodont.* **30**, 128–134. https://doi.org/10.1111/jopr.13231 (2021).
64. Kelly, E. Fatigue failure in denture base polymers. *J. Prosthet. Dent.* **21**, 257–266. https://doi.org/10.1016/0022-3913(69)90289-3 (1969).
65. Koshino, H., Hirai, T., Ishijima, T. & Ohtomo, K. Influence of mandibular residual ridge shape on masticatory efficiency in complete denture wearers. *Int. J. Prosthodont.* **15**, 295–298 (2002).
66. Slagter, A. P., Bosman, F. & Van der Bilt, A. Comminution of two artificial test foods by dentate and edentulous subjects. *J. Oral Rehabil.* **20**, 159–176. https://doi.org/10.1111/j.1365-2842.1993.tb01599.x (1993).
67. Haraldson, T., Karlsson, U. & Carlsson, G. E. Bite force and oral function in complete denture wearers. *J. Oral Rehabil.* **6**, 41–48. https://doi.org/10.1111/j.1365-2842.1979.tb00403.x (1979).
68. Borie, E. et al. Maximum bite force in elderly Indigenous and Non-Indigenous denture wearers. *Acta Odontol. Latinoam.* **27**, 115–119. https://doi.org/10.1590/S1852-48342014000300003 (2014).
69. Lindquist, L. W., Carlsson, G. E. & Hedegård, B. Changes in bite force and chewing efficiency after denture treatment in edentulous patients with denture adaptation difficulties. *J. Oral Rehabil.* **13**, 21–29. https://doi.org/10.1111/j.1365-2842.1986.tb01552.x (1986).
70. Pereira de Caxias, F. et al. Micheline Dos Santos, D. Effects of rehabilitation with complete dentures on bite force and electromyography of jaw and neck muscles and the correlation with occlusal vertical dimension. *Clin. Oral Investig.* **25**, 4691–4698. https://doi.org/10.1007/s00784-021-03783-1 (2021).
71. Ryniewicz, W., Bojko, Ł., Machniewicz, T. & Ryniewicz, A. M. Strength Tests of the Polymers Used in Dental Prosthetics. *Archive of Mechanical Engineering*; ; *vol. 65; No 4; 515–525* 2018. 2018. (2018).
72. Heath, M. R. The effect of maximum biting force and bone loss upon masticatory function and dietary selection of the elderly. *Int. Dent. J.* **32**, 345–356 (1982).
73. Takamiya, A. S., Monteiro, D. R., Marra, J., Compagnoni, M. A. & Barbosa, D. B. Complete denture wearing and fractures among edentulous patients treated in university clinics. *Gerodontology* **29**, e728–734. https://doi.org/10.1111/j.1741-2358.2011.00551.x (2012).
74. Shakir, S., Jalil, H., Khan, M. A., Qayum, B. & Qadeer, A. Causes and types of denture fractures - a study. *Pakistan Oral Dental Journal* **37**, 634–637 (2017).
75. Lamb, D. J., Ellis, B. & van Noort, R. The fracture topography of acrylic dentures broken in service. *Biomaterials* **6**, 110–112. https://doi.org/10.1016/0142-9612(85)90073-0 (1985).
76. Hertzberg, R. W. *Fatigue of Engineering Plastics*; Academic Press: New York, ; ISBN 978-0-12-343550-7. (1980).
77. Praveen, B. et al. Comparison of impact strength and fracture morphology of different heat cure denture acrylic resins: an in vitro study. *J. Int. Oral Health*. **6**, 12–16 (2014).
78. Faot, F., Panza, L. H. V., Garcia, R. C. M. R. & Cury, A. A. D. B. Impact and flexural Strength, and fracture morphology of acrylic resins with impact modifiers. *Open. Dent. J.* **3**, 137–143. https://doi.org/10.2174/1874210600903010137 (2009).
79. Tan, X. et al. Palatal radicular groove morphology of the maxillary incisors: A case series report. *J. Endod.* **43**, 827–833. https://doi.org/10.1016/j.joen.2016.12.025 (2017).
80. Shpack, N., Dayan, T., Mass, E. & Vardimon, A. D. Labial cervical vertical groove (LCVG) distribution and morphometric characteristics. *Arch. Oral Biol.* **52**, 1032–1036. https://doi.org/10.1016/j.archoralbio.2007.05.007 (2007).
81. Kishi, M. Experimental studies on the relation between area and displacement of loading surfaces in connection with displaceability in the mucosa of edentulous alveolar ridge under pressure. *Shika Gakuho Dent. Sci. Rep.* **72**, 17–45 (1972).
82. Bhattacharjee, B., Saneja, R., Singh, A., Dubey, P. K. & Bhatnagar, A. Peri-Implant stress distribution assessment of various attachment systems for implant supported overdenture prosthesis by finite element Analysis – A systematic review. *J. Oral Biol. Craniofac. Res.* **12**, 802–808. https://doi.org/10.1016/j.jobcr.2022.09.002 (2022).
83. Kümbüloğlu, Ö., Koyuncu, B., Yerlioğlu, G., Al-Haj Husain, N. & Özcan, M. Stress distribution on various Implant-Retained bar overdentures. *Mater. (Basel)*. **15**, 3248. https://doi.org/10.3390/ma15093248 (2022).
84. Barão, V. A. R., Delben, J. A., Lima, J., Cabral, T. & Assunção, W. G. Comparison of different designs of Implant-Retained overdentures and fixed Full-Arch Implant-Supported prosthesis on stress distribution in edentulous Mandible – A computed Tomography-Based Three-Dimensional finite element analysis. *J. Biomech.* **46**, 1312–1320. https://doi.org/10.1016/j.jbiomech.2013.02.008 (2013).
85. Frolo, M., Řehounek, L., Jíra, A., Pošta, P. & Hauer, L. Biomechanical analysis of palateless splinted and unsplinted maxillary Implant-Supported overdentures: A Three-Dimensional finite element analysis. *Mater. (Basel)*. **16**, 5248. https://doi.org/10.3390/ma16155248 (2023).
86. Gonda, T., Maeda, Y., Walton, J. N. & MacEntee, M. I. Fracture incidence in mandibular overdentures retained by one or two implants. *J. Prosthet. Dent.* **103**, 178–181. https://doi.org/10.1016/S0022-3913(10)60026-1 (2010).
87. (PDF) Viscoelasticity of Human Oral Mucosa: Implications for Masticatory Biomechanics. ResearchGate. (2025). https://doi.org/10.1177/0022034510396881
88. Sadr, K., Alipour, J. & Heidary, F. Finite element analysis of Soft-Lined mandibular complete denture and its supporting structures. *J. Dent. Res. Dent. Clin. Dent. Prospects.* **6**, 37–41. https://doi.org/10.5681/joddd.2012.009 (2012).
89. Barão, V. A. R., Assunção, W. G., Tabata, L. F., de Sousa, E. A. C. & Rocha, E. P. Effect of different mucosa thickness and resiliency on stress distribution of Implant-Retained Overdentures-2D FEA. *Comput. Methods Programs Biomed.* **92**, 213–223. https://doi.org/10.1016/j.cmpb.2008.07.009 (2008).
90. Kawano, F., Asaoka, K., Nagao, K. & Matsumoto, N. Effect of viscoelastic deformation of soft tissue on stresses in the structures under complete denture. *Dent. Mater. J.* **9**, 70–79123. https://doi.org/10.4012/dmj.9.70 (1990).

Acknowledgements

We would like to express our gratitude to Muhammad Ibn-Hashim Al-Ansari Ansari, Anahid W. Medjahed, and

Grzegorz Jania for their valuable discussions and for sharing their expertise during this research.

Author contributions

Y.M., J.Z., and H.L. performed the research, wrote the main manuscript text, and prepared the figures. All authors reviewed the manuscript.

Funding

This work was supported by the Researchers Supporting Project (BKM: 10/010/BKM25/1252) at the Silesian University of Technology, Poland. This research was also partially funded by European Funds, co-financed by the Just Transition Fund, through the project "Comprehensive Support for the Development of the Joint Doctoral School and Scientific Activities of Doctoral Students Related to the Needs of the Green and Digital Economy – Silesian University of Technology" (Project No. FESL.10.25-IZ.01-07E7/23). .

Declarations

Competing interests

The authors declare no competing interests.

Additional information

Correspondence and requests for materials should be addressed to Y.M. or J.Ż.